School of Pharmacy[1], Ningxia Medical University; Ningxia Engineering and Technology Research Center for Modernization of Hui Medicine & Key Lab of Hui Ethnic Medicine Modernization[2], Ministry of Education; General Hospital of Ningxia Medical University[3], Yinchuan, Ningxia, China

Glabridin nanosuspension for enhanced skin penetration: formulation optimization, *in vitro* and *in vivo* evaluation

WP. Wang[1,2], J. Hu[1], H. Sui[1,2], YS. Zhao[1,2], J. Feng[1], C. Liu[1,3]

Received September 17, 2015, accepted December 12, 2015

Chen Liu, General Hospital of Ningxia Medical University, 804 Shengli Street, Yinchuan, Ningxia 750004, P.R. China
657656264@qq.com

Pharmazie 71: 252–257 (2016) *doi: 10.1691/ph.2016.5152*

Glabridin, a polyphenolic flavonoid from licorice, has inspired great interest for its antioxidant, anti-inflammatory and skin-lightening activities. However, low water solubility and poor stability of glabridin impedes its topical application in cosmetic products and therapies of dermal diseases. The purpose of this study was to develop a nanosuspension formulation of glabridin to improve its skin permeation. Glabridin nanosuspensions were prepared using anti-solvent precipitation-homogenization method, and Box-Behnken design was adopted to investigate the effects of crucial formulation variables on particle size and to optimize the nanosuspension formulation. The optimal formulation consisted of 0.25% glabridin, 0.47% Poloxamer 188 and 0.11% Polyvinylpyrrolidone K30, and the obtained nanosuspension showed an average particle size of 149.2 nm with a polydispersity index of 0.254. Furthermore, the nanosuspension exhibited significantly enhanced drug permeation flux of glabridin through rat skin with no lag phase both *in vitro* and *in vivo*, compared to the coarse suspension and physical mixture. The glabridin nanosuspension showed no significant particle aggregates and a drug loss of 5.46% after storage for 3 months at room temperature. With its enhanced skin penetration, the nanosuspension might be a more preferable formulation for topical administration of poorly soluble glabridin.

1. Introduction

Glabridin (Glab) is a polyphenolic flavonoid compound derived from the root of licorice (*Glycyrrhiza glabra* L.; Fabaceae) (Fuhrman et al. 1997). Glab is well-known for its beneficial effects on the skin including antioxidant (Carmeli et al. 2008), anti-inflammatory (Park et al. 2010), antimicrobial (Gupta et al. 2008), radical-scavenging, and especially skin-lightening activities. Previous studies have reported that Glab can filter ultraviolet light and retard melanogenesis in skin by inhibiting tyrosinase activity (Gillbro and Olsson 2011; Deshmukh and Poddar 2012). Generally, Glab is consumed as a constituent of licorice extract, rather than as a single chemical entity. For example, as one of the licorice extracts enriched in Glab, Glabridin-40 is now widely used in cosmetic products (Simmler et al. 2013). However, the dermatologic application of Glab and Glab-enriched extracts has been hampered due to its low solubility in water, poor skin permeability and stability issues (Yokota et al. 1998; Ao et al. 2010). Previous reports have proposed the nanoemulsion and prodrug-based approaches to improve the skin absorption of Glab and its stability in formulations (Hsieh et al. 2012; Jirawattanapong et al. 2009). Yet the skin penetration performance of these formulations remains unknown.

Nanosuspensions, also called nanocrystals, are colloidal dispersions of active compounds with crystal size less than 1 μm (Müller and Peters 1998). The size reduction will lead to a dramatic increase in effective surface area, and thus enhance drug solubility and dissolution. (Shaal et al. 2010). As a result, the preparation of nanosuspensions has become one of the most important strategies to improve the absorption of the poorly soluble drugs. Although drug nanocrystals can be administered through various routes (Merisko-Liversidge and Liversidge 2008; Liu et al. 2012), most of the published articles and marketed products are dedicated to improve the oral bioavailability of hydrophobic drugs as nanosuspension (Zhai et al. 2014). Until now, a few published articles have confirmed the effectiveness of nanocrystal technology for enhanced dermal bioavailability of lipophilic drugs, such as rutin (Petersen 2006), hesperidin (Romero et al. 2015), diclofenac (Pireddu et al. 2015), tretinoin (Lai et al. 2013), ibuprofen (Yuan and Capomacchia 2013) and caffeine (Zhai et al. 2014). Therefore, the application of nanosuspension technology to Glab formulation could potentially promote drug permeation through the stratum corneum of human skin and hence improve the dermal pharmacological action of Glab. To the best of our knowledge, there has been no previous detailed publication related to the fabrication and evaluation of Glab nanosuspension for dermal administration.

In the present study, attempts were made to prepare Glab nanosuspensions using nanoprecipitation method. The nanosuspension formulation was optimized by means of Box-Behnken design (BBD), and then evaluated on particle size and stability. The permeation performance of Glab nanosuspension through rat skin was examined to explore the potential use of Glab nanosuspension in topical formulations.

2. Investigations, results and discussion

2.1. Analysis of response surfaces

As shown in Table 1, the particle size of Glab nanosuspensions from the 17 experimental runs varied from 151 nm to 235 nm. These data were then used to calculate the coefficients r^2, predicted r^2 and adjusted r^2 of the linear, two-factor (2F) interaction and quadratic equation. The results in Table 2 show that the quadratic model adequately represented the experimental data with a coefficient of multiple determinations (r^2) of 0.9781. Therefore, the quadratic equation of the response surface was adopted to predict the particle size of nanosuspensions.

The effects of the model terms and associated p values for all three responses were analyzed by ANOVA and summarized in Table 3. The polymer concentration (X_2), the ratio of aqueous phase to organic phase (X_3), their interactive terms (X_1X_2, X_1X_3), and poly-

Table 1: Experimental particle size obtained from the BBD (mean ± S.D, $n = 3$)

Formulation	Factors			Y (nm)
	X_1 (%)	X_2 (%)	X_3 (%)	
1	0.6	0.1	20	219.1 ± 17.5
2	0.4	0.2	10	199.5 ± 16.5
3	0.5	0.3	10	171.3 ± 9.0
4	0.5	0.2	20	161.8 ± 9.1
5	0.5	0.2	20	156.5 ± 5.9
6	0.6	0.2	30	211.2 ± 8.4
7	0.5	0.1	30	183.7 ± 6.6
8	0.5	0.2	20	163.2 ± 8.1
9	0.6	0.3	20	213.8 ± 9.2
10	0.5	0.2	20	167.9 ± 11.1
11	0.6	0.2	10	157.8 ± 7.3
12	0.4	0.3	20	234.6 ± 18.7
13	0.4	0.1	20	201.2 ± 8.5
14	0.5	0.3	30	205.7 ± 10.3
15	0.5	0.2	20	166.8 ± 17.4
16	0.5	0.1	10	151.2 ± 4.0
17	0.4	0.2	30	203.2 ± 8.5

Table 2: Results of model summary statistics analysis for responses

Model	Y (particle size)		
	r^2	Adjusted r^2	Predicted r^2
Linear	0.2491	0.07584	-0.3267
2F	0.3405	-0.05512	-1.3693
Quadratic	0.9781	0.95012	0.7597

Table 3: Quantitative factor effects and associated p value for the responses

Parameters	Y (Particle size)		
	Sum of Squares	Degree of freedom	p value
Model	10622.84	9	< 0.0001*
X_1	167.44	1	0.0615
X_2	616.01	1	0.0037*
X_3	1922.00	1	0.0001*
X_1X_2	374.42	1	0.0127*
X_1X_3	617.52	1	0.0037*
X_2X_3	0.90	1	0.8749
X_1^2	4994.88	1	< 0.0001*
X_2^2	1599.82	1	0.0002*
X_3^2	95.30	1	0.1373

***p<0.05, significant values**

nomial model of surfactant and polymer concentrations (X_1, X_2) were identified as significant model terms ($p < 0.05$). The final mathematical equation of the fitted model is given below:

$Y = 163.24 - 4.57X_1 + 8.78X_2 + 15.50X_3 - 9.68X_1X_2 + 12.43X_1X_3 + 0.47X_2X_3 + 34.44X_1^2 + 19.49X_2^2 - 4.76X_3^2$ ($r^2 = 0.9747$)

This equation possessed a correlation coefficient (r^2) value of 0.9747, indicating that 97.47% of the sample variation in particle size was ascribed to the experimental variables studied. The F value of 68.18 indicated the significance of the model ($p < 0.0001$), and the lack of fit F value of 2.53 implies that the lack of fit is not significant ($p = 0.1962$). Thus, the fitted equation can be used to predict the best formulation for Glab nanosuspensions.

2.2. Optimization of formulation components for Glab nanosuspension

In addition, we generated a series of three-dimensional (3D) response surfaces to further investigate the interaction and quadratic effects of the variables on the response. Figure 1 was generated by varying two of the independent variables within the experimental range while holding another one constant at the central point. As shown in Fig. 1, the average particle size of the freshly prepared nanosuspensions increased with the growth of volumetric ratio of aqueous phase and organic phase in a nonlinear mode, i.e. the size increased from 151 nm at a low ratio (10) to 211 nm at a high ratio (30). It is apparent that a small size can be obtained at relatively higher concentrations of organic phase, when the final Glab concentration in the mixture of aqueous and organic phases was fixed at 0.25% (w/v). During the process of nanosuspension formation, supersaturation is the crucial driving force to determine both the nucleation rate and the diffusion-controlled growth rate. Due to greater supersaturation at a higher ratio of aqueous phase to organic phase, the growth rate and agglomeration rate was more dominant than nucleation rate, and then led to larger crystals.

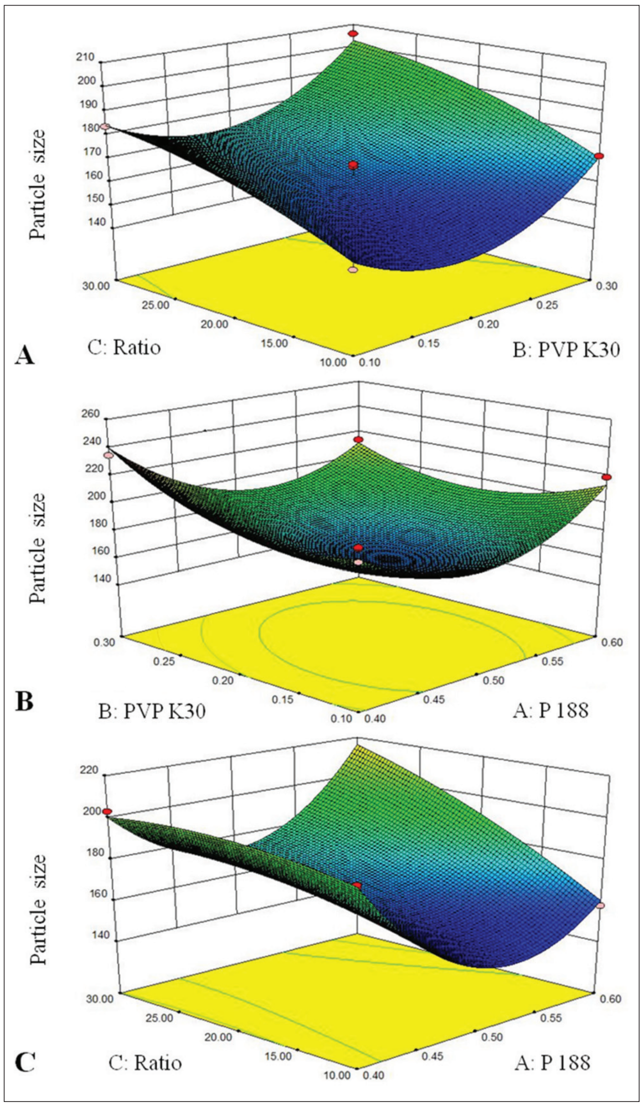

Fig.1: Three-dimensional contour plot of the effect of independent factors on response of particle size Y. (A) X_2 and X_3 on response Y, (B) X_1 and X_2 on response Y, (C) X_1 and X_3 on response Y.

In this study, polyvinylpyrrolidone (PVP K30) was applied as a steric stabilizer for Glab nanosuspensions, and its concentration in the aqueous phase also showed a significant effect ($p < 0.05$) on particle size. Theoretically, PVP can be liable to cover the surface

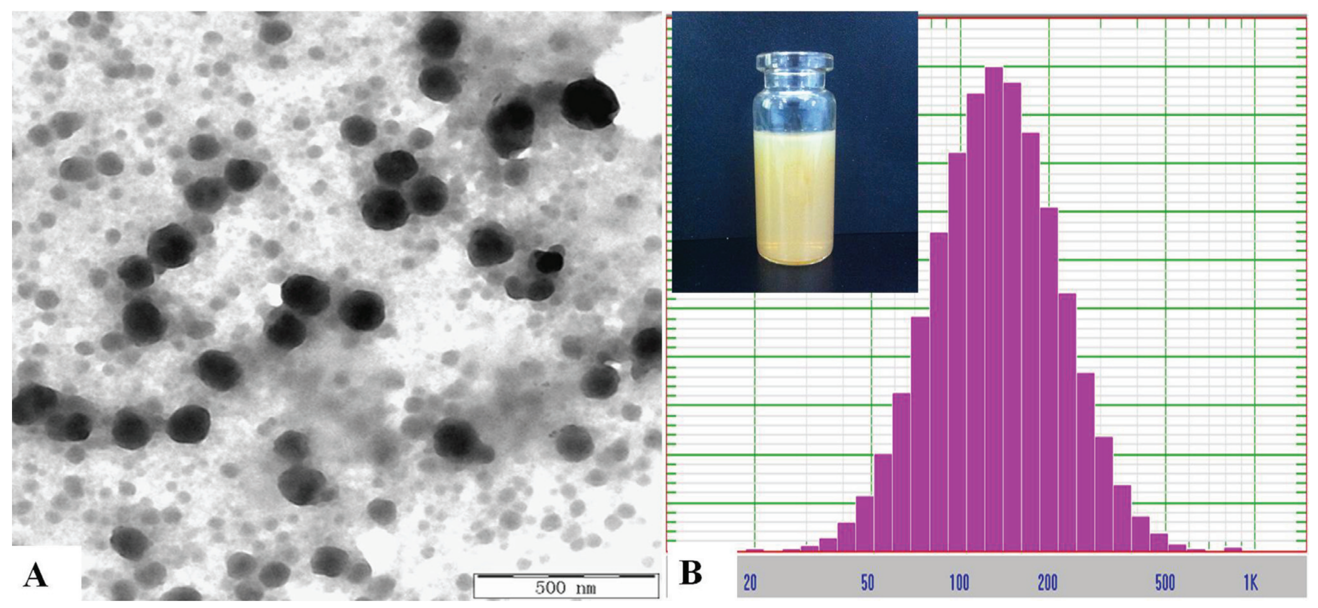

Fig.2: TEM image (A, Scale bar: 500 nm) and appearance particle distribution (B) of the optimized Glab nanosuspension.

of the newly formed crystals and to offer a mechanical barrier against crystallization, which can further occupy the adsorption sites and prevent the growth and agglomeration of the crystals (Hao et al. 2015). Insufficient polymer would not provide complete surface coverage and result in rapid crystal growth and agglomeration, while excess polymer would enhance the attraction among colloidal particles by increasing osmotic pressure and inhibit diffusion between the aqueous and organic phases by thickening the cloak during the nanoprecipitation process, and finally give rise to larger crystals (Thorat et al. 2012).
The formulation of Glab nanosuspensions was further optimized with minimum particle size, using the equation and the responds in response surfaces. The optimal composition was determined as follows: 0.47% Poloxamer 188 (P188), 0.11% PVP K30, and a 10:1 volume ratio of aqueous phase to organic phase. Glab nanosuspension prepared with the optimal formulation exhibited a mean particle size of 149.2 nm, which was in good agreement with the value predicted by the model (158.4 nm). The results confirmed that the model was effective and reliable for predicting the impact of formulation composition on the particle size of Glab nanosuspensions.

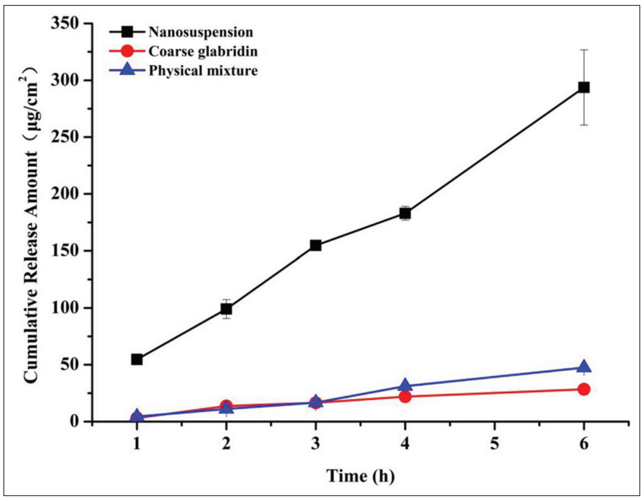

Fig.3: In vitro permeation of Glab through rat skin (n = 3).

2.3. Morphology and particle size analysis

Figure 2A shows the morphology of Glab crystals under Transmission Electron Microscope (TEM). Particles with spherical shape were observed under TEM, and their sizes extended from 50 to 200 nm. The particle size distribution and the appearance of the Glab nanosuspension of optimal formulation are shown in Fig. 2B. Glab nanosuspension showed a yellow translucent appearance to the naked eyes. The size distribution was unimodal and typically extended from 50 to 400 nm, the mean particle size was approximately 140 nm with a polydispersity index (PI) of 0.254, which was consistent with TEM photos.

Table 4: Permeation parameters of the suspensions in vitro skin permeation test (mean ± S.D, n = 3)

Formulation	J_{ss} (μg/cm^2)/h	$P\times10^3$ (cm/h)	T_{Lag} (h)
Nanosuspension	48.94 ± 5.51*	21.56*	—
Physical mixture	7.92 ± 0.13	3.49	0.708
Coarse suspension	4.74 ± 0.39	1.90	—

***p<0.05, statistical significance compared with coarse suspension**

2.4. In vitro skin permeation study

Glab penetration through rat skin was evaluated under *in vitro* conditions using Franz vertical diffusion cells covered by parafilm. The cumulative amounts of drug permeated per centimeter squared against time are displayed in Fig. 3 and the permeation parameters are listed in Table 4. The J_{ss} of Glab nanosuspension was significantly increased by approximately 10.3- and 6.2-fold, when compared with that of the coarse suspension and the physical mixture, respectively. In addition, the J_{ss} of physical mixture was 1.7-fold higher than that of the coarse suspension. The highest P value and no lag phase were also observed for the nanosuspension formulation.
As an active pharmaceutical ingredient with high lipophilicity (log $P \approx 3.25$), Glab is expected to possess excellent affinity with skin lipid, thus the release rate of drug becomes a key factor limiting its permeation rate through skin. Since a nanosuspension can significantly improve the dissolution of poorly soluble drugs by size reduction corresponding to increased surface area, an enhanced permeation rate was commonly observed (Shen et al. 2015). For the physical mixture, the reduced particle size and the presence of

ethanol (< 10%) and P188 (0.47%, w/v) can facilitate drug release, and improve the performance of skin permeation as well.

2.5. *In vivo drug penetration test*

Figure 4 summarizes the amounts of Glab per skin area after treated with different suspensions. The nanosuspension formulation showed the highest penetration during the test period, while the coarse suspension showed the lowest skin delivery. The penetration performance of drug-loaded solution was predominantly affected by drug concentration gradient into the skin. Since the solution with dispersed drug nanocrystals has higher saturation solubility due to size reduction, the nanocrystals would enhance skin penetration due to a higher concentration gradient. In addition, it is reported that follicular penetration could make a major contribution to dermal uptake, and nanocrystals would accumulate more in hair follicles than pure solutions, which would make further contribution to the increased penetration (Patzelt et al. 2011; Lademann et al. 2008).

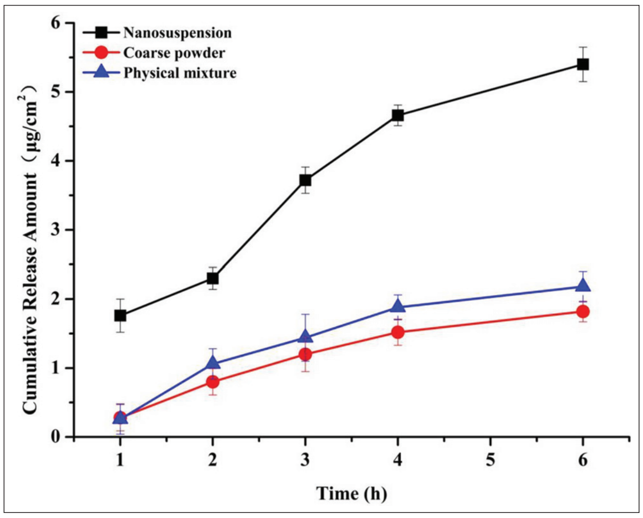

Fig.4: In vivo skin permeation of Glab-loaded formulations (*n* = 5).

In this study, the amounts of drug delivered through rat skin after treatment with nanosuspensions was the highest at all time intervals among the three formulations and no lag time was observed. Skin penetration was significantly increased by using nanocrystal technology. These results supported the fact that a topical formulation of Glab nanosuspension could be a great choice for a rapid onset and prolonged duration of action.

2.6. *Stability test*

Stability of three batches of Glab nanosuspensions was also investigated. As shown in Table 5, their particle size remained stable

Table 5: The stability of Glab nanosuspension at room temperature (mean ± S.D, *n* = 3)

Time (days)	Size (nm)	PI	DL (%)
0	142.2 ± 14.3	0.254 ± 0.033	0.238 ± 0.044
30	141.0 ± 7.4	0.224 ± 0.078	0.235 ± 0.059
60	149.9 ± 20.6	0.302 ± 0.099	0.230 ± 0.042
90	153.4 ± 6.7	0.297 ± 0.021	0.225 ± 0.011

after storage for three months at room temperature. PI was slightly increased, indicating crystal growth or agglomeration. However, some approaches can be applied to avoid the Ostwald ripening effect. The addition of hydrophilic polymers (Carbopol, HPMC etc.) into the nanosuspension formulation could further improve the physical stability of crystals (Agarwal and Bajpai 2013).

In a previous study of Yu's group (Ao et al. 2010), the degradation of Glab was accelerated as the increasing temperature and relative humidity, the drug loss reached 5.9% and 12.7% after storage for 5 and 10 days under the condition of 25ºC and 75% (relative humidity), respectively. In the present work, Glab content only showed a reduction of 5.46% from 0.238% to 0.225% during the 90 days storage, despite of the large surface of the nanosuspension in contact with the water phase. In addition, the introduction of some antioxidant agents and other additives into the formulation would further improve the chemical stability of Glab. Therefore, further studies are needed.

2.7. *Conclusion*

The present study showed that Glab nanosuspension with narrow particle size range can successfully be prepared by anti-solvent precipitation and homogenization techniques. The BBD experimental design helped in probing the optimal formulation and in identifying the key factors that affect the particle size of nanosuspensions. The formation of nano-scale crystals enhanced both *in vitro* and *in vivo* skin permeation of Glab, and the obtained nanosuspension was relatively stable for a short-term storage. The present study can open a window for topical application of formulations loaded with Glab nanosuspension in cosmetic products for skin whitening or in the treatment of dermatological disorders like melasma (Callender et al. 2011).

3. Experimental

3.1. *Materials*

Glab (40%, w/w) was procured from Jingzhu Biology Technology Co., Ltd. (Nanjing, China). Poloxamer 188 (P188) was from Chineway Pharmaceutical Tech Co., Ltd. (Shanghai, China). Polyvinylpyrrolidone (PVP K30) was purchased from Boai Nky Pharmaceuticals Ltd. (Jiaozuo, China). Ethanol was obtained from Damao Chemical Reagent Factory (Tianjin, China). All other reagents used were of analytical grade. All solutions were freshly made using double distilled water at room temperature.

3.2. *Preparation of Glab nanosuspensions*

The antisolvent precipitation-homogenization method was used to prepare Glab nanosuspensions (Pireddu et al. 2015). In a typical procedure, Glab was completely dissolved in ethanol to form the organic solution. The antisolvent phase was obtained by dispersing a specific concentration of surfactant and/or polymer in water. Then, the organic phase was rapidly introduced into the antisolvent phase under homogenization at 9500 rpm for 2 min using an Ultra Turrax T18 homogenizer (IKA, Germany). The nano-scale drug suspensions with yellowish opalescence appearance were formed immediately in the process of nanoprecipitation.

3.3. *Experimental design*

Preliminary studies (Yue et al. 2013; Zhang et al. 2014) have demonstrated that the critical variables, which significantly affect the physicochemical properties of the obtained nanosuspensions, include the concentration of surfactant (P188, X_1) and polymer (PVP K30, X_2) in aqueous phase, and the volume ratio of aqueous phase to organic phase (X_3). Therefore, the response surface methodology and a 3-factor-3-level BBD, generated by Design-Expert software (Version 8.0.6.1) were explored to probe the optimal variables and to study the effect of these three independent factors on particle size (Y) of Glab nanosuspensions. The experiments are listed in Table 6.

Table 6: Independent variables used in the BBD

Independent variables	Levels		
	-1	0	1
X_1=Level of P188 (%)	0.4	0.5	0.6
X_2=Amount of PVP K30 (%)	0.1	0.2	0.3
X_3=Ratio of aqueous phase to organic phase	10	20	30
Dependent variables	Constraints		
Y=Particle size	Minimize		

3.4. *Particle size analysis*

The nanosuspensions were diluted with water, and their particle size and size di

Nicomp, Santa Barbara, CA, USA) using the light scattering technique. Each analysis lasted 120 s and was performed at 25 °C with a detection angle of 90°.

3.5. *Transmission electron microscopic observation*

One drop of nanosuspension was placed on a carbon-coated copper grid and dried at room temperature. The morphology of nanocrystals was observed under TEM (H-7650, Hitachi, Japan).

3.6. *HPLC determination of Glab*

The concentration of Glab in samples was determined using L-2000 liquid chromatography system (Hitachi, Japan) equipped with L-2200 auto-injection device. The chromatographic analysis was carried out with a reverse phase YMC-Pack Pro C18 column (5 μm, 4.6×250 mm). The mobile phase was a mixture of acetonitrile and 0.44% glacial acetic acid solution (62:38, v/v) at a flow rate of 1.0 mL/min and the detection was performed at 282 nm using L-2455 UV–VIS detector (Hitachi, Japan) (Shanker et al. 2007).

3.7. *In vitro permeation through rat skin*

The permeation of Glab from suspensions was determined by using a vertical Franz diffusion cell (RYJ-6A, Tianjin, China) with an effective diffusion area of 2.89 cm^2 and the receptor volume of 6.5 mL, according to the method described by Kalhapure with some modifications (Kalhapure and Akamanchi 2013). The full-thickness skin was excised from the abdomen of male Sprague-Dawley rats (7-9 weeks old, 200±20 g), and then mounted on the receptor compartment with the stratum corneum side facing upwards into the donor compartment. A mixture of acetonitrile and pH 7.4 phosphate buffer saline (60:40, v/v) was used as the receptor medium to maintain a sink condition, and was continuously stirred using a magnetic stirrer at 500 rpm and maintained at 32±1 °C to simulate the skin temperature throughout the experiment. Then, 2 mg dose of Glab, in the form of different suspensions (0.25%, w/v), was loaded onto the skin surface in the donor compartment and covered with parafilm paper on top of the cell. Aliquots (each of 1mL) were withdrawn at predetermined time intervals (1, 2, 3, 4, 5 and 6 h), and immediately replaced by an equal volume of fresh medium. All the collected samples were then filtered through a 0.22 μm syringe filter (Lab Instruments Co., Ltd., Shanghai, China) and analyzed for drug content by the HPLC method described above. The total amount of drug penetrated through the unit diffusion surface (Qt, μg/cm^2) versus time (t, h) was plotted. The steady-state fluxes (J_{ss}, μg/cm^2/h) were calculated from the slope of the linear plot and the lag time (T_{lag}) was determined by extrapolating the cumulative mass per unit area versus time profile at apparent steady state to the abscissa. The apparent permeability coefficients (P, cm/h) were calculated by dividing the steady-state flux (J_{ss}) with the initial donor drug concentration (C_0, μg/mL).

3.8. *In vivo skin delivery study*

Fifteen male Sprague-Dawley rats (7-9 weeks old, 200±20 g) were obtained from the Laboratory animal center of Ningxia Medical University (Yinchuan, China). All animals were maintained in a specific pathogen-free environment at 23±2 °C with free access to water. All procedures were approved by the Animal Research Ethics Committee, General Hospital of Ningxia Medical University.

In vivo skin delivery studies were performed according to the methods described by Tiossi with some modifications (Tiossi et al. 2014). The dorsal hair of rats was shaved using electric and hand razors, and then a piece of filter paper (1 cm^2) pre-absorbed with 30 μL of Glab-loaded formulations was stuck to the shaved skin. At the end of the preset time intervals, the filter paper was removed from the skin, and 3 strips of adhesive tape were consecutively applied and removed. The filter paper and the tapes were cut into small pieces, transferred into a test tube and extracted with 4 mL ethanol for 2 times. The resulting solution was collected and centrifuged at 4000 rpm for 2 min. The supernatant was filtered through 0.22 μm membrane and quantified by HPLC. The total drug amount of penetrated through and remained within the skin was obtained by substrate the residual drug from the original drug amount applied.

3.9. *Short term stability test*

For stability investigations, Glab nanosuspensions were stored at room temperature for three months. The particle size and PI of samples were analyzed on the day of preparation and after 30, 60 and 90 days of storage. Appearance observation was performed to investigate the presence of agglomerations or sedimentations. Drug content was monitored to elucidate the chemical stability issues.

3.10. *Statistical analysis*

All results are expressed as the mean and standard deviation. SPSS software (version 17.0) was used to analyze the data. ANOVA and Student's t-test was used to investigate the statistical differences. The $p < 0.05$ was considered as statistically significant.

Acknowledgements: This work was supported by the National Natural Science Foundation of China (81360644, 81160521) and the Natural Science Foundation of Ningxia (NZ15145).

References

Al Shaal L, Müller RH, Keck CM (2010) Preserving hesperetin nanosuspensions for dermal application. Pharmazie 65: 86-92.

Ao M, Shi Y, Cui Y, Guo W, Wang J, Yu L (2015) Factors influencing glabridin stability. Nat Prod Commun 5: 1907-1912.

Callender VD, St Surin-Lord S, Davis EC, Maclin M (2011) Postinflammatory hyperpigmentation Etiologic and Therapeutic Considerations. Am J Clin Dermatol 12: 87-99.

Carmeli E, Harpaz Y, Kogan NN, Fogelman Y (2008) The effect of an endogenous antioxidant glabridin on oxidized LDL. J Basic Clin Physiol Pharmacol 19: 49-63.

Deshmukh K, Poddar SS (2012) Tyrosinase inhibitor-loaded microsponge drug delivery system: new approach for hyperpigmentation disorders. J Microencapsul 29: 559-568.

Fuhrman B, Buch S, Vaya J, Belinky PA, Coleman R, Hayek T, Aviram M (1997) Licorice extract and its major polyphenol glabridinprotect low-density lipoprotein against lipid peroxidation. Am J Clin Nutr 66: 267-275.

Gillbro JM, Olsson MJ (2011) The melanogenesis and mechanisms of skin-lightening agents-existing and new approaches. Int J Cosmet Sci 33: 210-221.

Gupta VK, Fatima A, Faridi U, Negi AS, Shanker K, Kumar JK, Rahuja N, Luqman S, Sisodia BS, Saikia D, Darokar MP, Khanuja SP (2008) Antimicrobial potential of Glycyrrhiza glabra roots. J Ethnopharmacol 116: 377-380.

Hao J, Gao Y, Zhao J, Zhang J, Li Q, Zhao Z, Liu J (2015) Preparation and optimization of resveratrol nanosuspensions by antisolvent precipitation using Box-Behnken design. AAPS PharmSciTech 16: 118-128.

Hsieh CW, Li PH, Lu IC, Wang TH (2012) Preparing glabridin-in-water nanoemulsions by high pressure homogenization with response surface methodology. J Oleo Sci 61: 483-489.

Jirawattanapong W, Saifah E, Patarapanich C (2009) Synthesis of glabridin derivatives as tyrosinase inhibitors. Arch Pharm Res 32: 647-654.

Kalhapure RS, Akamanchi KG (2013) Oleodendrimers: a novel class of multicephalous heterolipids as chemical penetration enhancers for transdermal drug delivery. Int J Pharm 454: 158-166.

Lademann J, Knorr F, Richter H, Blume-Peytavi U, Vogt A, Antoniou C, Sterry W, Patzelt A (2008) Hair follicles--an efficient storage and penetration pathway for topically applied substances. Summary of recent results obtained at the Center of Experimental and Applied Cutaneous Physiology, Charité-Universitätsmedizin Berlin, Germany. Skin Pharmacol Physiol 21: 150-155.

Lai F, Pireddu R, Corrias F, Fadda AM, Valenti D, Pini E, Sinico C (2012) Nanosuspension improves tretinoin photostability and delivery to the skin. Int J Pharm 458: 104-109.

Liu Y, Xie P, Zhang D, Zhang Q (2012) A mini review of nanosuspensions development. J Drug Target 20: 209-223.

Merisko-Liversidge EM, Liversidge GG (2008) Drug nanoparticles: formulating poorly water-soluble compounds. Toxicol Pathol 36: 43-48.

Müller RH, Peters K (1998) Nanosuspensions for the formulation of poorly soluble drugs I. Preparation by a size-reduction technique. Int J Pharm 160: 229-237.

Park SH, Kang JS, Yoon YD, Lee K, Kim KJ, Lee KH, Lee CW, Moon EY, Han SB, Kim BH, Kim HM, Park SK (2010) Glabridin inhibits lipopolysaccharide-induced activation of a microglial cell line, BV-2, by blocking NF-kappaB and AP-1. Phytother Res 24: S29-S34.

Patzelt A, Richter H, Knorr F, Schäfer U, Lehr CM, Dähne L, Sterry W, Lademann J (2011) Selective follicular targeting by modification of the particle sizes. J Control Release 150: 45-48.

Petersen R (2006) Nanocrystals for use in topical cosmetic formulations and method of production thereof. US patent 60/8866233.

Pireddu R, Sinico C, Ennas G, Marongiu F, Muzzalupo R, Lai F, Fadda AM (2015) Novel nanosized formulations of two diclofenac acid polymorphs to improve topical bioavailability. Eur J Pharm Sci 77: 208-215.

Romero GB, Chen R, Keck CM, Müller RH (2015) Industrial concentrates of dermal hesperidin smartCrystals®-production, characterization & long-term stability. Int J Pharm 482: 54-60.

Shanker K, Fatima A, Negi A, Gupta V, Darokar M, Gupta M, Khanuja S (2007) RP-HPLC Method for the Quantitation of Glabridin in Yashti-madhu (Glycyrrhiza glabra). Chromatographia 65: 771-774.

Shen CY, Li RS, Shen BD, Shen G, Wang LQ, Zheng J, Li XR, Min HY, Han J, Yuan HL (2015) Influence of drug physicochemical characteristics on in vitro transdermal absorption of hydrophobic drug nanosuspensions. Drug Dev Ind Pharm 20: 1-9.

Simmler C, Pauli GF, Chen SN (2013) Phytochemistry and biological properties of glabridin. Fitoterapia 90: 160-184.

Thorat A, Dalvi S (2012) Liquid antisolvent precipitation and stabilization of nanoparticles of poorly water soluble drugs in aqueous suspensions: Recent developments and future perspective. Chem Eng J 181-182: 1-34.

Tiossi RF, Da Costa JC, Miranda MA, Praça FS, McChesney JD, Bentley MV, Bastos JK (2014) In vitro and in vivo evaluation of the delivery of topical formulations containing glycoalkaloids of Solanum lycocarpum fruits. Eur J Pharm Biopharm 88: 28-33.

Vuddanda PR, Mishra A, Singh SK, Singh S (2015) Development of polymeric nanoparticles with highly entrapped herbal hydrophilic drug using nanoprecipitation technique: an approach of quality by design. Pharm Dev Technol 20:579-587.

Yokota T, Nishio H, Kubota Y, Mizoguchi M (1998) The inhibitory effect of glabridin from licorice extracts on melanogenesis and inflammation. Pigment Cell Res 11: 355-361.

Yuan X, Capomacchia AC (2013) Influence of physicochemical properties on the in vitro skin permeation of the enantiomers, racemate, and eutectics of ibuprofen for enhanced transdermal drug delivery. J Pharm Sci 102: 1957-1969.

Yue P, Li Y, Wan J, Wang Y, Yang M, Zhu W, Wang C, Wang H (2013) Process optimization and evaluation of novel baicalin solid nanocrystals. Int J Nanomedicine 8:2961-73.
Zhai X, Lademann J, Keck CM, Müller RH (2014) Nanocrystals of medium soluble actives-novel concept for improved dermal delivery and production strategy. Int J Pharm 470: 141-150.
Zhang Q, Hong T, Wei S, Sui H, Wang W (2014) Preparation Technology of Baicalin Nanocrystallines. Chine J Experim Trad Med Form 20: 14-18.